DESIGN ANALYSIS OF STATIONS AND INTERSECTIONS OF A HIGH-CAPACITY PERSONAL RAPID TRANSIT NETWORK

K. Thangavelu, D. S. Berry, and B. M. Shaefer, Northwestern University

This paper describes an effort to develop geometric designs for high-capacity personal rapid transit links, stations, and intersections and to predict and evaluate their performance under quasi-synchronous control at different design and operating conditions. The system assumed 1-way routes and vehicle accelerations and decelerations only on the off-lines. The geometric design of off-lines at stations and intersections considers recommended normal and centripetal acceleration and jerk rates, allowable radius of curvature, required maneuver zone length, and required capacity of the off-line and the line spacing chosen. Typical conditions for a large urban area are considered. In the PRT system, vehicle queues are formed on the upstream and downstream sides of station platforms and intersection turns. The modeling, analysis, and simulation of these queues are described. The excess capacities and the sizes of queuing zones needed can be obtained from simulation results for stations and intersections of different capacities. The resulting average waiting time, the probability of vehicle rejection on the upstream side, the probability of forced switching to prevent the stopping of vehicles on the downstream side, and the achievable guideway density are given as functions of design and operating parameters. The possible trade-offs among design capacity, traffic density, length of queuing zone, and user costs involved at stations and intersections are discussed.

•THE CONCEPTS of people movers, personal rapid transit systems, and dual-mode vehicle systems originated in the last decade as solutions to urban transportation problems. The personal rapid transit (PRT) system is proposed as an alternative to automobile use on urban arterial streets. These systems use automobile-sized vehicles on grade-separated guideways and are operated by electronic controls and computers. Complete network traffic control enables efficient routing, scheduling, empty-car dispatching, and balanced loading of the network.

During the past few years various strategies for network traffic control have been proposed: synchronous cycle concept, synchronous slot concept, quasi-synchronous concept, and multizone zone-synchronous concept. The selected network control philosophy affects the system performance—station and intersection use, waiting times and delays in the system, average speed of travel, average trip length, possible guideway density—and also the control, communication, and computer requirements for the vehicle and the Network subsystems.

The ongoing research work at Northwestern University consists of designing a hypothetical PRT network for possible application in a large metropolitan area and simulating its operation under various network control strategies to study the effect of control strategy on system performance. This paper deals with the design of stations and intersections for a PRT network under quasi-synchronous control.

ASSUMPTIONS

1. Vehicles operate at uniform speeds over 1-way guideways. The speed selected results in an average speed of travel higher than that possible with automobiles.
2. The stations and intersections are located on off-line guideways, which are designed with consideration to system effectiveness and geometric limitations.

3. The vehicles accelerate and decelerate only in the off-lines.
4. The network spacing and station distribution permit easy accessibility of the system in the CBD and inner-city areas and accessibility from the developed portion of land in the outer rings.
5. The vehicles are automobile-sized and can carry 4 to 6 persons. The average occupancy is 1.5 persons.
6. The vehicle spacing and control systems provide for acceptable levels of safety.
7. The network meets the personal travel demand for automobiles and bus transit expected within a typical large metropolis in 1990.

ABBREVIATIONS AND NOTATION

The abbreviations and notation used in this paper are given below.

a_m = maximum centripetal acceleration;
C = guideway capacity, in vehicles/hour;
C_s = station capacity, in vehicles/hour;
C_r = capacity ratio between main line and HIS;
$C_e = C/C_r$, theoretical capacity of HIS;
C_v = velocity ratio between main line and HIS;
f = tire friction factor;
H_D = vehicle interarrival time or headway, in s-cycles;
HIS = high impedance section;
J = smallest integer such that (when C_r involves a fraction) JC_r is an integer;
K = spacing factor;
L_{tr} = trigger zone length, in feet;
LCC = local control computer;
L_s = station spacing, in miles;
LVS = local vehicle sensors;
$m = T_M/[(C_r - 1)J]$, maximum number of vehicles accommodated in the upstream and downstream queues after Markovian renewal process;
n_B = average number of vehicles block circling;
N_{cc} = time to communicate, compute, and command vehicle switching, in s-cycles;
N_{CMS} = travel time from switch to merge node on main line, in s-cycles;
N_{Cr} = minimum travel time on downstream side from HIS exit to merge node, in s-cycles;
N_{CSN} = maximum number of slots from switch to slot sensor;
N_s = number of stations/square mile;
$N\Delta$ = number of slots to be checked to ensure forced switching with given probability;
p_B = probability of vehicle being observed block circling;
p_f = probability of forced switching;
p_r = probability of vehicle rejection at switch;
$p_{SL} = (1 - U_f) + p_v$, probability of an empty slot being observed on the main line;
p_v = probability of vehicle being observed seeking switching from main line to HIS or merging from HIS to main line during an s-cycle;
$q_r = (1 - P_r)$, probability of a vehicle being switched at the switch;
R = allowable radius of curvature;
$R_a = p_r/q_r$, average number of block-circling rounds;
S = spacing between vehicles;
$S_L = S + L_v$, length of slot, in feet;
S_L/V = s-cycle, the time for slot to cross any point on main line;
S_r = slot ratio, the reciprocal of ρ_D;
S_t = slot time, in seconds;
t_a = average interarrival time between vehicles on HIS;
t_b = average block-circling time;
t_{wq} = average waiting time in queue;
t_{wt} = average total waiting time;
T_A = trigger advance;

T_M = maximum number of triggers provided;
T_{MN} = maximum number of triggers required to allow waiting vehicle to occupy slot vacated by forced switching;
T_{MX} = maximum allowable number of triggers on the downstream side;
T_N = trigger used by the vehicle—vehicle waiting time in s-cycles;
TR = turn ratio, the ratio between smaller number of vehicles turning off a line and larger number of vehicles turning off cross line;
U_f = guideway density;
U_{fs} = guideway density downstream of switch;
U_{fx} = guideway density upstream of switch and on line off which smaller number of vehicles turn;
V = main-line velocity;
V_s = HIS velocity;
$\rho_D = p_v/p_{SL}$, density for downstream queue; and
ρ_s = HIS density.

HYPOTHETICAL PRT NETWORK DESIGN

Main Lines

The hypothetical PRT network was designed to meet the traffic demand for the Chicago metropolitan area in 1990 as forecast by the Chicago Area Transportation Study (CATS) for the finger plan of the Northeastern Illinois Planning Commission (1). The CATS area in the 1956 study consisted of 8 rings. Each ring was treated as a uniform area and the internal trips, external trips, and through trips made in each ring by automobiles and bus transit were obtained. Based on trip lengths, peak-hour factors, and vehicle occupancy, the loaded vehicle flow rates per mile width of corridor per direction were obtained.

The maximum possible flow is less than the theoretical capacity of the main guideway because of the gaps left between vehicles to enable other vehicles to enter from stations and intersections. Hence, the main-line traffic density or the volume-capacity ratio is 0.6 to 0.85 at peak times. Several of the vehicles on the guideway will be empty, proceeding to stations to pick up passengers or returning from stations after dropping passengers. Thus, the effective use of the guideway is 0.6 or less at peak times.

The first PRT system should have a theoretical guideway capacity of 3 to 4 times the capacity of a freeway lane to justify the efforts, time, and funds required for research and development. This requires vehicle headways of about 0.5 sec and results in an actual loaded-vehicle flow rate of about twice the freeway lane volume. With this capacity, line spacings of ¼ mile in the CBD, ½ mile in the inner city, and 1 mile in outer rings meet the traffic demands in the Chicago area. Speeds of 20, 40, and 60 mph respectively may be considered for the above areas, based on average speeds of travel desired and the off-line lengths needed at stations and intersections.

Stations

If 1 station is placed on each link, 100 percent of the area in the CBD and inner-city areas and 39 percent of the area in the outer rings will be within ¼-mile walking distance from stations. If 2 stations are placed on each link, the accessible area can be increased to 64 percent, but the guideway speed will have to be decreased to 40 to 50 mph in the outer rings.

The peak-hour passenger load per station can be estimated from the traffic demand data. Excess empty vehicles must be provided to stations to serve stochastic passenger arrivals. Stations must be designed with excess vehicle-handling capacity to accommodate stochastic vehicle arrivals. Thus, effective use depends on station and vehicle use and is of the order of 0.6 or less. The station theoretical capacity is based on proper vehicle occupancy and effective use.

The ratio of theoretical guideway capacity to the station capacity affects queue characteristics and station performance. This ratio varies in the range of 8 to 18 for the

CATS area PRT network. Table 1 gives the guideway and station capacities and the capacity ratio for CATS area rings (2).

GEOMETRIC DESIGN OF STATIONS AND INTERSECTIONS

The geometry of the off-lines at stations and intersections has been considered by Dais (3, 4). These consist of a switch, a maneuver zone, a high-impedance section (HIS), a rear maneuver zone, and a merge (Figs. 1 and 2).

Switch and Merge

Vehicles exit the main line through the switch and enter the main line through the merge. These consist of 2 Euler spiral pairs. A lateral displacement of 12 ft between center lines of the main line and the off-line is reasonable for a vehicle width of 7 ft. The lateral displacement produced depends on allowable maximum centripetal acceleration and jerk rates. Since superelevation would be difficult to provide for the switch and the merge, all of the lateral acceleration must be balanced by the tire friction and will be experienced by passengers. For a maximum centripetal jerk of 0.125 g/sec, as observed by the Japanese National Railway (5), the a_m will be 0.14 g. The switches and the merges are designed with a_m varying from 0.14 g at 20 to 40 mph to 0.11 g at 60 mph, as recommended by Moyer and Berry (6). At higher speeds, 2 small circular arc segments are used in between the wind-unwind segments of the Euler spirals to obtain the necessary lateral displacement.

Maneuver Zone

The maneuver zones consist of 3 overlapping regions: trigger zone, speed-change zone, and queuing zone.

Speed-Change Zone—The speed-change zones (ramps) provide for vehicle deceleration from V to V_s on the upstream side of the HIS and vehicle acceleration from V_s to V on the downstream side of the HIS. These use trapezoidal deceleration and acceleration profiles. Normal acceleration and jerk rates of 0.25 g and 0.25 g/sec respectively are used for the ramps.

Queuing Zone—The capacity of the HIS off-line is much less than that of the main line. The stochastic vehicle arrival results in queue formation in front of the HIS. The station and turn performances can be measured in terms of probability of vehicle rejection at the switch, the average waiting time in queue, the number of vehicles block circling from a given station, and the total delays on the upstream side. All these depend on C_r, ρ_s for the queuing process, and the queue size provided.

Vehicles move at the speed of the HIS on the queuing zone. On the downstream side, the queuing zone is provided immediately after the HIS. The larger the relative velocity is between the main line and the HIS, the smaller the queuing zone length will be.

Trigger Zone—The trigger zone is provided at the switch end of the maneuver zone on the upstream side and the HIS end of the maneuver zone on the downstream side. Triggers, typically electrical loops, are provided at equal spacings on the trigger zone. The trigger spacing depends on the velocity ratio between the main line and the HIS and the length of slot on the main line. Triggers actuate vehicle deceleration circuits and initiate deceleration at proper points on the upstream side and acceleration at proper points on the downstream side. The triggers are operated by the local control computer, which receives communication from local vehicle sensors located on the main line (Fig. 1).

HIS

A platform is the HIS at stations, and the turn is the HIS at intersections. The platforms are linear and use moving belts. People use the belt to deboard and board the vehicle as it moves slowly along the platform. Belt speed is synchronized with that of the vehicles at the platform. Belt stations result in high capacity with small platform size and queue-zone length.

Table 1. PRT system guideway and station design factors.

Ring	Peak-Hour Person Trips/Direction/Mile Width of Corridor (persons/hour)	Lines/Mile Width of Corridor	Speed (mph)	S_L	S_L	C	K	N_s	L_s	C_s	C_r
CBD	13,350	2	20	15	1/2	7,200	0.116	32	1/4	720	10
1	9,200	1	40	25	5/12	8,640	0.106	8	1/2	960	9
2	9,270	1	40	25	5/12	8,640	0.106	8	1/2	864	10
3	9,690	1	40	25	5/12	8,640	0.106	8	1/2	720	12
4	9,435	1	40	25	5/12	8,640	0.106	8	1/2	720	12
5	5,040	1	40	30	1/2	7,200	0.141	8	1/2	480	15
6	3,300	1/2	40	30	1/2	7,200	0.141	4	1/2	480	15
7	2,580	1/2	60	45	1/2	7,200	0.118	2 to 4	1 to 1/2	480	15

Figure 1. PRT off-line station.

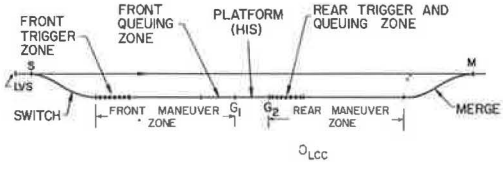

Figure 2. Plan view of PRT intersection.

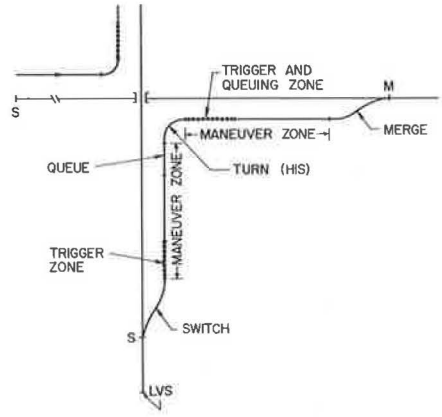

Figure 3. Triggering on upstream and downstream sides.

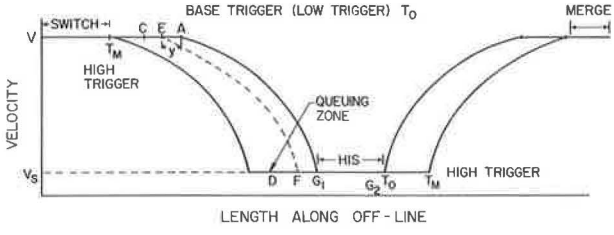

Figure 4. Numbering triggers on upstream and downstream sides.

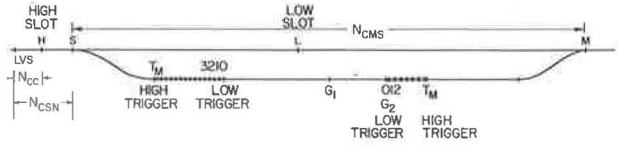

Given the proper spacing between vehicles on the platform, the required vehicle and belt velocity can be obtained for the given station capacity. The platform length is chosen so that it provides for a platform time of 15 to 25 sec and is an integral multiple of slot length at the platform.

The turn consists of an arc with Euler spiral transitions at either end. In high-capacity PRT systems, the turns cannot be designed with the same capacity as that of the main line, for this requires a high turn velocity and hence a large radius of curvature and superelevation, which is unacceptable to the urban situation. The allowable radius of curvature in the urban areas is less than 40 ft for the turns. A tire friction factor of 0.2 g was considered realistic to allow for wet guideway conditions and rubber-tired wheels. If R = 35 ft and f = 0.2 g, the allowable maximum turn velocity is 15 ft/sec, which results in a theoretical turn capacity of 4,500 vehicles/hour and slot lengths of 12 ft at the turn. This capacity is considered sufficient in all rings, for only a fraction of main-line vehicles seek to turn at any intersection.

Lower speeds of turning can be used with lower turn capacities and will result in decreased acceleration and jerk during turns. C_r is the ratio of theoretical main-line capacity to the theoretical turn capacity, in vehicles/hour. For CATS area intersections, capacity ratios of 1.6, 2, and 3 were considered.

QUEUING PROCESS ON UPSTREAM SIDE OF HIS

Vehicle Arrival on Main Line

In PRT systems using synchronous and quasi-synchronous control, the vehicles move in discrete slots of length $S_L = S + L_V$. The time taken for a slot to cross any point on the main line is S_L/V and is called an s-cycle.

Vehicle observation by the LVS is a Bernoulli process. The probability of a vehicle being observed at LVS seeking switching from the main line to HIS is $p_v = \rho_s/C_r$. The number of vehicles seeking switching during n s-cycles is given by a binomial distribution of parameters n and p_v. C_s is a measure of the service rate, while C_r is a measure of service time in s-cycles.

For the Bernoulli vehicle arrival process, the vehicle interarrival time n has a geometric distribution. The probability of n, $p(n) = p_v q_v^{n-1}$, where $q_v = (1 - p_v)$.

Vehicle Maneuver on Upstream Side

A vehicle switched to the off-line moves at main-line speed on the switch. If it need not wait in queue, it traverses the trigger zone at the same speed and decelerates from A to HIS gate G_1, as shown in Figure 3.

Suppose another vehicle on the main line with vehicle 1 is switched. If H_D is less than C_r, the vehicle has to wait in queue. If vehicle 2 starts deceleration at the same point as vehicle 1, it will collide with vehicle 1 before reaching G_1. If vehicle 2 starts deceleration at the same instant as vehicle 1, it will reach G_1, $H_D C_v$ s-cycles after vehicle 1. This will result in low use of the HIS capacity, for the HIS can admit 1 vehicle every C_r s-cycles. By properly choosing the point where vehicle 2 starts deceleration, one can make the vehicles enter the HIS at intervals of C_r s-cycles without collision.

The distance of the point of initiation of deceleration from A is given by

$$y = \frac{S_L}{(C_v - 1)} (C_r - H_D) \tag{1}$$

C_r may be integer or noninteger. Choose a small integer J such that JC_r is an integer. The triggers are located at spacings of $S_L/[(C_v - 1)J]$. The value of y can then be given in terms of number of triggers counted.

The trigger spacing and the time taken to traverse a trigger spacing at normal speed before triggering are both called a trigger. Therefore,

$$1 \text{ trigger} = \frac{S_L}{(C_v - 1)J} \text{ ft} = \frac{S_t}{(C_v - 1)J} \text{ sec} \tag{2}$$

The triggers are numbered as shown in Figure 4. The lowest trigger is called the base trigger.

When the vehicle advance, $C_r - H_D$, is positive, triggering has to be advanced: $T_A = (C_r - H_D)J$. Given the trigger used by the Nth vehicle, that used by the (N + 1) vehicle is given by

$$\begin{aligned} T_{N+1} &= T_N + T_A = T_N + J(C_r - H_D) && \text{if } T_N \neq 0 \\ T_{N+1} &= T_N + T_A = J(C_r - H_D) && \text{if } T_N = 0 \\ T_{N+1} &= T_N + T_A = 0 && \text{if } JH_D > (T_N + JC_r) \end{aligned} \tag{3}$$

When JH_D is greater than $(T_N + JC_r)$, the vehicle interarrival time on HIS is greater than C_r s-cycles. T_M, the maximum number of triggers provided, is finite because of the cost of triggers and the trigger zone. If the trigger required by the vehicle is greater than T_M, the vehicle will be rejected at the switch.

Queuing Process on Upstream Side and Its Simulation

In Eq. 3, C_r is the service time and H_D is the vehicle interarrival time in s-cycles. Hence, T_N and T_{N+1} are the vehicle waiting time in terms of 1/J s-cycles for the queuing process involved. 1/J s-cycle may be called a cyclet. A cyclet may be used as a unit of time for the off-lines. The queue can be represented by the model M/D/1-F, FIFO, for the vehicle arrival is a Markovian process (the vehicle arrival is an independent process, being a Bernoulli process), the service time is constant, and the queue size is finite.

The main HIS characteristics of interest are p_r and t_{wt}, both of which should be minimized. The vehicle is rejected when the required waiting time exceeds T_M or when the queue is full. If M is the maximum line length provided for, then $p_r = P_M$, the probability that there are M vehicles in the line. At stations the rejected vehicles go around the block, increasing the travel time and the trip length and unnecessarily loading the guideway.

The probability of rejection and the average waiting time in queue depend on C_r, ρ_s for the queuing process, and T_M. The maximum length of queue increases linearly with T_M. Vehicles having a minimum headway of 1 s-cycle require $(C_r - 1)J$ triggers. Hence, T_M may be provided as integral multiples of $J(C_r - 1)$ so that an integral number of successive vehicles may be accommodated in the queue after the renewal process.

The queuing process was simulated to determine the probability of vehicle rejection, the average waiting time in queue, and the vehicle interarrival time on the HIS. Experiments were conducted with C_r values of 8, 12, and 15 for stations and 1.6, 2, and 3 for intersections. ρ_s for the queuing process was varied from 0.6 to 0.9, and the value of m was selected in the range of 2 to 8.

Figure 5 shows the flow diagram for the simulation model used. The program is written in FORTRAN IV for execution on the CDC 6400 computer. Each experiment was repeated for 10 independent runs. As a fixed number of 600 vehicles were switched to the off-line, the total number of vehicles received, the total number of vehicles rejected, the trigger used by each vehicle (and hence vehicle waiting time), the vehicle interarrival time at HIS gate G_1, and the number of rounds made by the vehicle before switching were noted. Also the number of vehicles block circling was noted at regular intervals of 60 s-cycles at stations. Hence, p_r, t_{wq}, t_a, and n_B were all calculated for each run. From the 10 independent observations made during the 10 runs, the mean values of p_r, t_{wq}, t_a, and n_B were obtained for each experiment. The total waiting time at stations was the sum of waiting time in queue and average block-circling time. The probability and cumulative probability distributions were also obtained.

Characteristics of Queuing Process

Probability of Rejection—Figure 6 shows the variation of p_r with m, C_r, and ρ_s at the station upstream side. p_r decreases at a decreasing rate as m and, hence, queuing zone lengths are increased. The law of decreasing return applies here. As ρ_s decreases,

Figure 5. Upstream operation simulation.

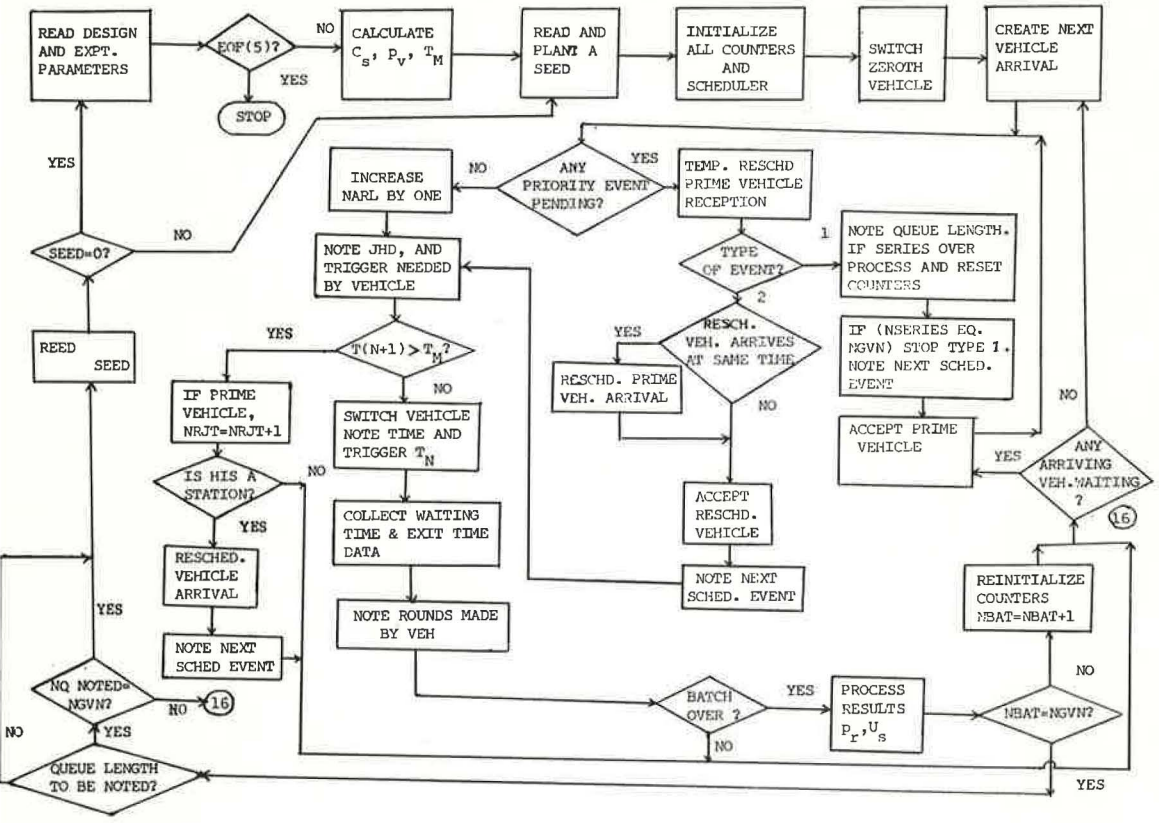

Figure 6. Variation of p_r at station on upstream side.

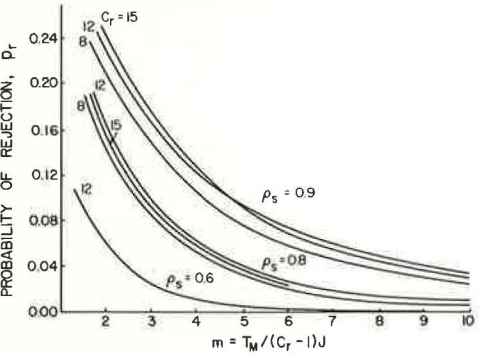

Figure 7. Variation of p_r at intersection.

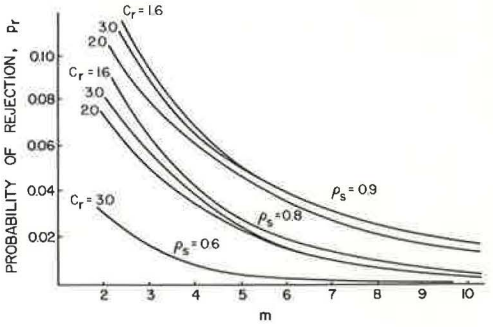

the average queue length and waiting time in queue decrease, and, hence, p_r decreases. At stations, p_r decreases as C_r decreases at $\rho_s = 0.9$ because of the increased service rate. At $\rho_s = 0.8$, p_r first increases and then decreases as C_r decreases.

The relations given by Saaty (7) were used to calculate p_r values for different values of m and ρ_s. These p_r values do not depend on C_r. The calculated p_r values lie within the range of p_r values observed at different capacity ratios during simulation.

A probability of rejection of 1 to 2 percent is acceptable at stations at peak time. A p_r value of 2 percent is obtained for $\rho_s = 0.8$ at m = 6 and for $\rho_s = 0.9$ at m = 12. Thus, higher values of ρ_s require large trigger zone lengths. A ρ_s value of 0.8 is feasible for station operation at peak time. During the peak hour, the average ρ_s will be only 0.64 and, hence, p_r will be about 0.2 percent. m = 6 at $\rho_s = 0.8$ results in 6 vehicles being rejected during the peak 20 min in a busy high-capacity station. If m = 4 were used, $p_r = 0.055$ at $\rho_s = 0.8$, resulting in 14 vehicles being rejected during the peak 20 min at the busy station. The m values of 4 to 6 are reasonable for the stations. Higher values of m are not recommended because of decreasing benefits.

Figure 7 shows the variation of p_r at intersections. Use of noninteger capacity ratios results in increased probability of rejection. A p_r value of 1/40 is reasonable for intersections. This is achieved with m = 8 at $\rho_s = 0.9$ and m = 5 at $\rho_s = 0.8$. Since the intersection downstream requires more triggers, a ρ_s value of 0.8 and m = 5 are recommended for all intersections. The selected value of p_r results in a rejection of 20 vehicles during the peak 20 min in the inner city with $C_r = 3.0$. During the other 40 min of the peak hour, ρ_s is less than p_r is of the order of 0.006 to 0.008.

Number of Vehicles Block Circling From Station and Average Number of Rounds Made—At stations, the rejected vehicles block circle and return to the station. The observation of block-circling vehicles on the main line is a Bernoulli process. The number of vehicles block circling has a binomial distribution of parameters n and p_B, where n is the number of slots around the block and $p_B = p_v[p_r/(1 - p_r)]$.

A p_B value of 0.5 percent is allowable; i.e., the average number of vehicles block circling from a station may be 1/200 of the number of slots available around the block. Figures 8 and 9 show the variation of p_B with m, C_r, and ρ_s. At $\rho_s = 0.8$, $p_B = 0.35$ to 0.5 percent at m = 4 and $p_B = 0.1$ to 0.2 percent at m = 6. Thus, m = 4 to 6 is acceptable at stations. R_a values were both measured and computed from p_r; they vary with m, C_r, and ρ_s exactly as p_r. Average block-circling times were calculated from the R_a values measured. These are given in Table 2 for m = 4 to 6 and $\rho_s = 0.8$.

Average Waiting Time in Queue and Total Waiting Time—The variation of t_{wq} is shown in Figure 10. The queuing time increases as C_r, m, and ρ_s increase. It increases at a decreasing rate as m increases. The average queuing time is maximum for the infinite queue and is given by

$$W_q^* = (\rho_s/2)[C_r/(1 - \rho_s)] \quad (4)$$

t_{wt} at stations is the sum of average block-circling time and average queuing time. The variation of upstream total waiting time at stations is shown in Figure 11 for $\rho_s = 0.8$. The decreasing utility of additional triggers is evident above m = 6.

At stations, m = 4 results in total waiting time of 20 to 23 sec in the CBD and inner city and 30 sec in the outer rings. Assuming that acceptable t_{wt} is less than or equal to 30 sec, m = 4 is acceptable. At m = 6 and $\rho_s = 0.8$, t_{wt} is 13 to 17 sec in the CBD and inner city and 20 sec in the outer rings. Thus, m = 6 is sufficient for $\rho_s = 0.8$.

At intersections, m = 5 and $\rho_s = 0.8$ result in average queuing time of 0.87 s-cycles at $C_r = 1.6$, 1.46 s-cycles at $C_r = 2.0$, and 2.9 s-cycles at $C_r = 3$.

Possible Trade-Offs in Design of HIS

Stations and intersections can be designed with less excess capacity (higher capacity ratio) and a higher number of triggers or more excess capacity and a smaller number of triggers and hence smaller queue size. A third dimension is added by user costs, such as the average total waiting time and the inconvenience caused by the vehicle rejection at a switch. Thus, a trade-off is possible among HIS design and operating costs, trigger costs, and user costs involved.

Figure 8. Variation of p_B with m.

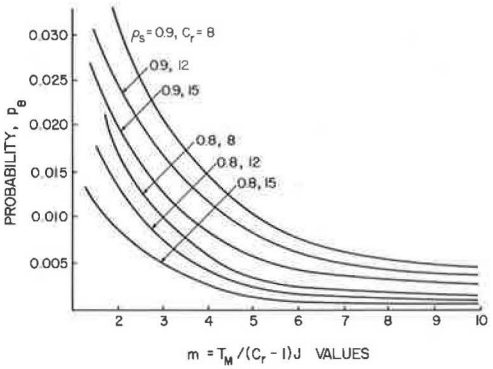

Figure 9. Variation of p_B with C_r.

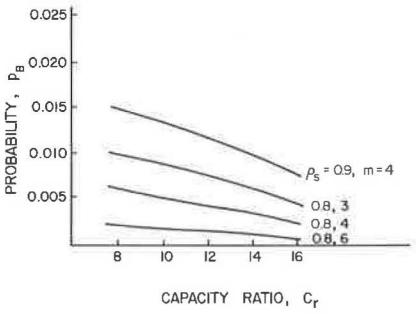

Table 2. Block-circling time on PRT network in CATS area.

Ring	Average Turn Time (s-cycles)	Main-Line Link (s-cycles)	Total Block-Circling Time (s-cycles)	R_a		t_o (sec)		C_r
				ρ_s = 0.8, m = 4	ρ_s = 0.8, m = 6	ρ_s = 0.8, m = 4	ρ_s = 0.8, m = 6	
CBD	56	54	440	0.062	0.025	13.65	5.5	10
1	75	72	588	0.059	0.024	14.45	5.87	9
2	75	72	588	0.062	0.025	15.2	6.13	10
3, 4	75	72	588	0.065	0.025	15.9	6.13	12
5	75	72	588	0.055	0.0225	13.5	5.5	18
6, 7	73	100	692	0.061	0.0225	21.1	7.8	15

Note: ρ_s = 0.9 at m = 7 has almost the same block-circling time as ρ_s = 0.8 at m = 4.

Figure 10. Variation of t_{wq} with C_r, m, and p_s.

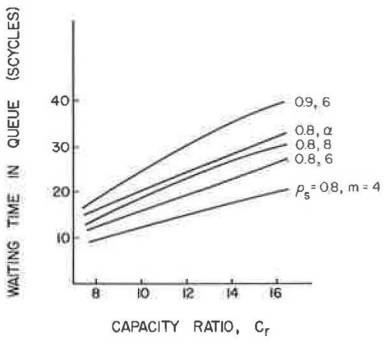

Figure 11. Variation of t_{wt} at station on upstream side.

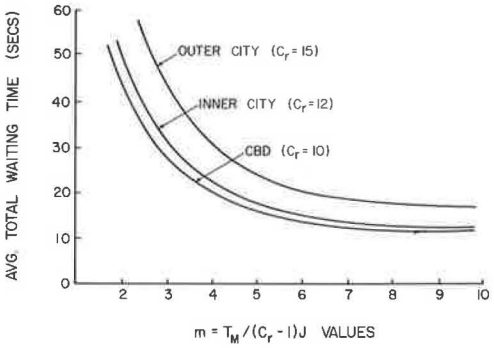

Figures 12, 13, and 14 show for the stations typical probability and cumulative probability distributions of the number of vehicles block circling, the waiting time in queue, and the vehicle interarrival time at the HIS. Similar curves were obtained for intersections. A fraction of the vehicles have constant interarrival time at the HIS, but others have geometrically distributed interarrival time with a minimum of $(JC_r + 1)$ cyclets.

QUEUING PROCESS ON DOWNSTREAM SIDE OF HIS

The vehicles in queue on the downstream side of the HIS are waiting for empty slots on the main line. The queuing is accomplished by the relative velocity between the main line and the off-line. The vehicle waiting and merging are exactly similar to vehicle merging on freeways.

Triggers are provided to initiate vehicle acceleration at different points on the queuing zone so that the vehicle catches its assigned slot on the main line. The triggers are numbered as shown in Figures 3 and 4.

Suppose a vehicle is triggered by the base trigger at HIS gate G_2. If the next vehicle arrives after H_{DS} s-cycles at the HIS exit and the available empty slot has a headway of H_D s-cycles on the main line with the slot used by the previous vehicle, then the position y of the point for initiation of vehicle acceleration from G_2 is given by

$$y = \frac{S_L}{(C_v - 1)} (H_D - H_{DS}) \tag{5}$$

If triggers are placed at spacings of $S_L/[(C_v - 1)J]$ ft, y is given in terms of number of triggers counted, as on the upstream side. If T_N is the trigger used for the Nth vehicle, then

$$\begin{aligned} T_{N+1} &= T_N + J(H_D - H_{DS}) && \text{if } T_N \neq 0 \\ T_{N+1} &= J(H_D - H_{DS}) && \text{if } T_N = 0 \\ T_{N+1} &= 0 && \text{if } JH_{DS} > (T_N + JH_D) \end{aligned} \tag{6}$$

Equation 6 is the recursive equation for waiting time in queue for the queuing process involved. The trigger used by the vehicle gives its waiting time in cyclets. The queue has a general distribution for vehicle interarrival times. The slot arrival on the main line is a Markovian process (Bernoulli process). The queue size is finite. Hence, the queue can be represented by the Model G/M/1-F, FIFO.

Vehicle Merging From Downstream Side

At intersections, let p_v be the probability of vehicle arrival at the exit of a high-density turn. The ratio between a smaller number of vehicles turning off a line and a larger number of vehicles turning off the cross line is the turn ratio. The probability of slots being observed for merging the larger number of vehicles is

$$p_{SL} = (1 - U_{fx}) + p_v \, TR \tag{7}$$

Hence, the traffic density ρ_D for the downstream queue is given by p_v/p_{SL}.

Because of the stochastic nature of vehicle and slot arrival, excess empty slots should be provided on the main line to enable easy vehicle merging. Hence, the ρ_D to be used is less than 1.0 at stations and intersections.

At intersections, C_r is small and a large number of vehicles seek to merge. TR will often be less than 1, and p_{SL} will be less on the line from which the smaller number of vehicles turn off. p_{SL} and s_r can be varied by varying U_{fx}. Thus, merging requirements at intersections determine the feasible guideway density.

The number of triggers provided on the downstream side is finite. Hence, the allowable vehicle waiting time is limited. If a vehicle does not get a slot within this time, it will have to be stopped on the downstream side. This may adversely affect

Figure 12. Probability of number of vehicles block circling.

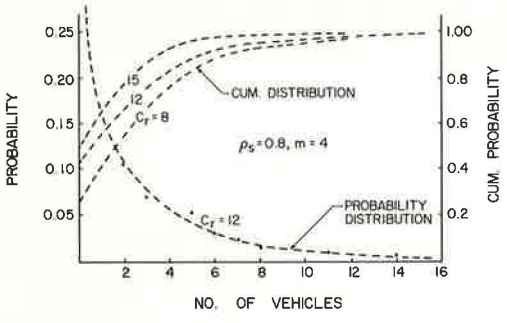

Figure 13. Probability of queuing time.

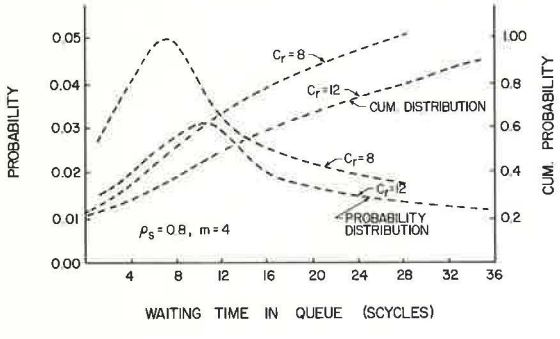

Figure 14. Probability of interarrival time in HIS.

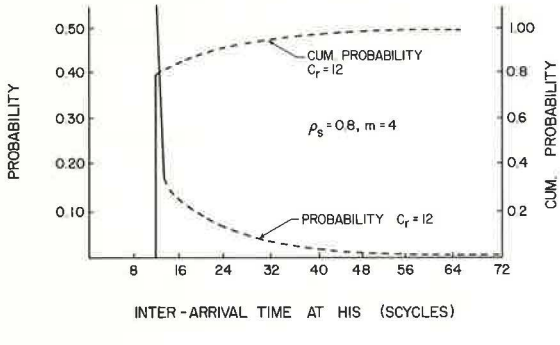

the HIS operation and result in undesirable vehicle rejection on the upstream side. A low-priority vehicle on the main line can be forced to switch to the off-line and its slot used to merge a vehicle stopped on the downstream side. If the LVS is located several slots before the switch, the LCC can be provided with information regarding the status of vehicles on several slots so that an empty vehicle may be selected for forced switching without any cost to the users.

Simulation of Downstream Queuing Process

Since the queuing process involved on the downstream side is difficult for analytical study, the required excess slots on the main line, the number of triggers to be provided on the downstream side, the probability of forced switching, and the feasible guideway traffic density were all determined by the simulation method. Experiments were conducted at different vehicle arrival rates by varying C_r and keeping ρ_s constant at 0.8. The vehicle interarrival times at HIS gate G_1 measured during upstream simulation were used to create vehicle arrival. Different numbers of triggers were chosen for the downstream side.

At intersections, ρ_D was varied from 0.7 to 0.9. The slot arrival was created, and the resulting p_f was measured during the merging process. Hence the acceptable combination of T_M and ρ_D for the downstream side was obtained. At intersections, choosing ρ_D determines the p_{SL} required. If TR is known, the required U_{fx} can be obtained. A p_f value of 1/80 is considered acceptable at intersections. This results in forced switching of about 10 vehicles during peak time at a busy intersection with a capacity ratio of 3.0.

At stations, the number of vehicles seeking to merge is small. However, the vehicle interarrival time is large, and hence, for the same values of ρ_D as used at intersections, the service time is large. This results in a long waiting time and hence a large number of triggers. Thus, stations require smaller values of ρ_D and larger slot ratios. The experiments were conducted by varying U_f on the upstream side of the station switch from 0.7 to 0.9. For different capacity ratios and constant ρ_s of 0.8, the resulting p_{SL} and ρ_D were measured as well as the p_f and average queuing time at different values of number of triggers provided. Based on an acceptable p_f value of 1/200 at stations, the required T_M was selected.

When forced switching is adopted, the downstream side should have a certain minimum number of triggers provided to allow time for the vehicle waiting to catch the slot emptied by forced switching. The minimum number of triggers is given by

$$T_{MN} = N_{CMS} + (N\Delta - 1) - N_{Cr} \tag{8}$$

The number of triggers used and the location of the slot sensor are also related. The maximum allowable number of triggers is given by

$$T_{MX} = N_{CMS} + N_{CSN} - N_{cc} - N_{Cr} \tag{9}$$

At stations and intersections, for different numbers of triggers, T_M for the upstream and downstream sides, N_{CMS}, N_{Cr}, and T_{MN} were calculated for all rings in the CATS area. The maximum available sensing space before stations and intersections was determined, and T_{MX} was obtained. These values are given in Table 3 for stations. The selected values of T_M lie in the range of T_{MN} to T_{MX}.

Let N_{CSL1} be the position of the slot from the merge node when vehicle 1 reaches the HIS exit. Therefore,

$$T_1 = N_{CSL1} - N_{Cr} \tag{10}$$

If H_{DS} is the headway between vehicles at HIS and H_D is the headway of the next available slot, then

$$N_{CSL2} = N_{CSL1} - H_{DS} + H_D$$

$$T_2 = N_{CSL2} - N_{Cr} \tag{11}$$

Table 3. Values of N_{Cr}, N_{CMS}, T_{MN}, and T_{MX} at station.

Region	Speed (mph)	N_{Cr} m	N_{Cr} Value	N_{CMS} m_1	N_{CMS} m_2	N_{CMS} Value	T_{MN} m_1	T_{MN} m_2	T_{MN} Value	T_{MX}
CBD	20.0	2	20	4	2	36	4	2	16	24
		3	21	4	3	37	4	3	16	
		4	22	6	3	39	6	3	16	
		6	23							
Inner city	35.8	2	30	4	2	46	4	2	16	26
		3	31	4	3	47	4	3	16	
		4	31	6	3	48	6	3	16	
		6	32							
Outer rings	50.0	2	30	4	2	42	4	2	12	24
		3	31	4	3	43	4	3	12	
		4	31	6	3	43	6	3	12	
		6	32							

Figure 15. Variation of p_f at stations.

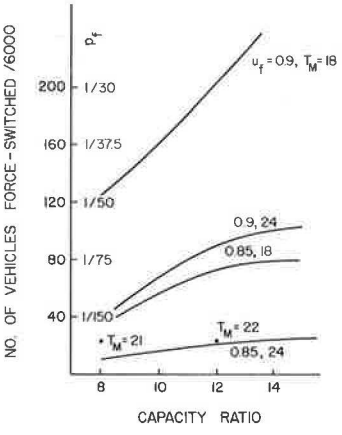

Figure 16. Variation of t_{wq} at stations on downstream side.

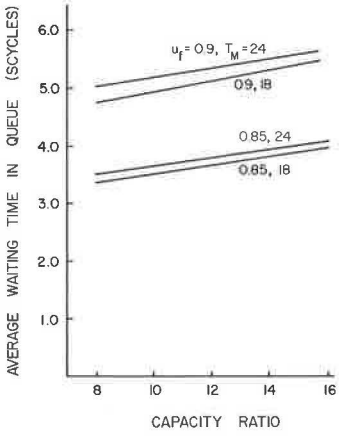

Figure 17. Number of vehicles forced to switch at intersections.

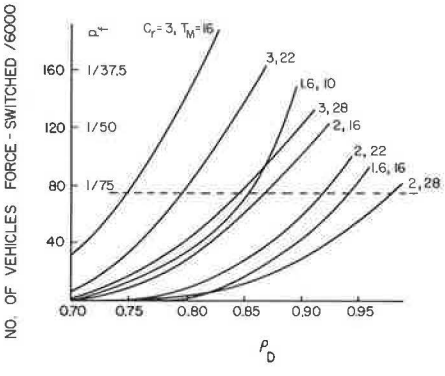

Figure 18. Average queuing time at intersections on downstream side.

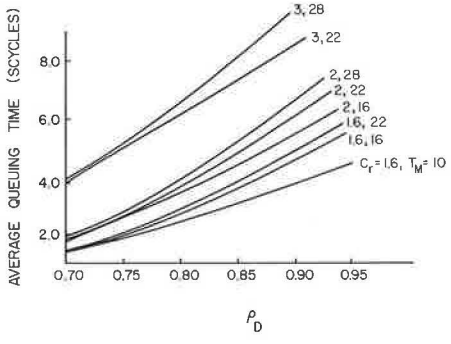

When $T_2 > T_M$, forced switching is adopted. The position of the first vehicle to be checked is given by

$$N_{CSLf} = \text{maximum of } (N_{CSL1} - H_{DS} + 1,\ N_{CMS} + 1) \quad (12)$$

Successive vehicles are checked to select a vehicle for forced switching.

Results of Simulation on Downstream Side

Figures 15 and 16 show the simulation results for the station downstream side. At stations, T_{MN} is 18 and T_{MX} is 24 when LVS is placed on the first slot on the intersection merge. A value of 20 to 24 triggers with $U_f = 0.85$ results in p_f of 0.004. Hence, at peak time only, 1 vehicle in 250 will require forced switching. About 2 to 3 vehicles will be accommodated in the downstream queue. The average vehicle waiting time is less than 2.0 sec.

At stations, values of m = 4 for upstream and m = 2 to 3 for downstream resulting in total trigger zone length of 70 to 80 ft are acceptable; m = 6 for upstream resulting in total trigger zone length of 104 ft is sufficient. On the upstream side, the length of the trigger zone is constant at all values of C_r, but the number of triggers varies. On the downstream side, the number of triggers increases slightly with C_r, but the trigger zone length decreases with an increase of C_r.

At intersections, T_{MN} varies from 17 to 25 and T_{MX} varies from 29 to 42. However, if the vehicles are allotted slots while they are on the turn, T_{MN} and T_{MX} can be decreased. T_M can then be low to decrease the downstream trigger zone length.

Experiments were conducted in which T_M was varied from 10 to 28 at different values of C_r and ρ_D. Figures 17 and 18 show the simulation results for the intersection downstream side.

p_f increases at an increasing rate as ρ_D is increased at all values of C_r and T_M. p_f is large at higher values of C_r because of higher interarrival time of vehicles and hence higher service time at the same ρ_D. p_f decreases as T_M is increased. A p_f value of 1/80 was selected as acceptable. The same value of p_f is obtained at higher values of ρ_D when the T_M used is large at a given C_r. At lower values of C_r, lower T_M and yet higher values of ρ_D can be used.

Table 4 gives the ρ_D values feasible and, hence, U_{fs} and U_{fx} values feasible at different values of T_M and C_r for p_f of 1/80. Higher values of ρ_D require more triggers and trigger zone length. A trade-off is possible between a higher value of T_M and a smaller value of U_{fx}.

U_{fx} values of 0.85 at TR = 0.75 and about 0.75 at TR = 0.5 were considered acceptable from guideway and intersection operation considerations. This requires a T_M value of 18 at all values of C_r. The resulting trigger zone length varies from 80 ft in the outer rings to 100 ft in the CBD at $C_r = 3.0$. At lower values of C_r, because of smaller relative velocity and velocity ratio, L_{tr} is higher. At $C_r = 1.6$, L_{tr} is 270 ft in the outer rings and 168 ft in the CBD.

Thus, use of larger capacity ratios and hence smaller capacities are preferred wherever possible. Also the variation of U_{fx} with TR is small at larger capacity ratios; hence, U_{fx} can be kept in the range of 0.70 to 0.85 for most intersections.

t_{wq} increases with ρ_D, almost linearly, and increases with T_M and C_r, as is expected. At the selected value of T_M, t_{wt} varies from 4.8 s-cycles at $C_r = 3.0$ to 5.5 s-cycles at $C_r = 1.6$. t_{wt} at an intersection varies from 7.7 s-cycles at $C_r = 3.0$ to 6.4 s-cycles at $C_r = 1.6$. At higher values of C_r, the time spent at the intersection off-line is slightly more. However, because of lower L_{tr} and hence the resulting higher feasible speeds of the main line, the travel time will be less at $C_r = 3.0$ than at $C_r = 1.6$.

Figure 19 shows the operating chart for intersections and stations. Suppose p_v for an intersection leg is given. It is shown as point A in Figure 19. ρ_D can be selected based on allowable p_f, available T_M on the downstream side, and C_r. Point B gives the required p_{sL}, and CD gives U_{fs}. If TR is known, U_{fx} can be obtained. If U_{fx} is given, the required TR and p_v for the cross leg can be obtained. If higher values of TR are used, U_{fx} can be large, as Figure 19 shows.

Table 4. Operating values at intersections for $p_f = 1/80$.

C_r	T_M	ρ_D	U_{fx} TR = 0.5	U_{fx} TR = 0.75	U_{fx} TR = 1.0	t_{wq}	L_{tr} CBD	L_{tr} Outer Rings
3.0	16	0.7475	0.7766	0.8433	0.9099	4.20	87.2	71.6
	22	0.795	0.7979	0.8646	0.9312	6.10	119.9	98.5
2.0	16	0.870	0.7402	0.8402	0.9402	4.70	213	114
	22	0.921	0.7657	0.8657	0.9657	6.60	293	157
	28	0.980	0.7919	0.8919	0.9919	9.30	373	187
1.6	16	0.945	0.7209	0.8459	0.9701	5.40	240	150
	22	1.00	0.7500	0.875	1.000	5.80	330	206

Figure 19. Intersection operating chart.

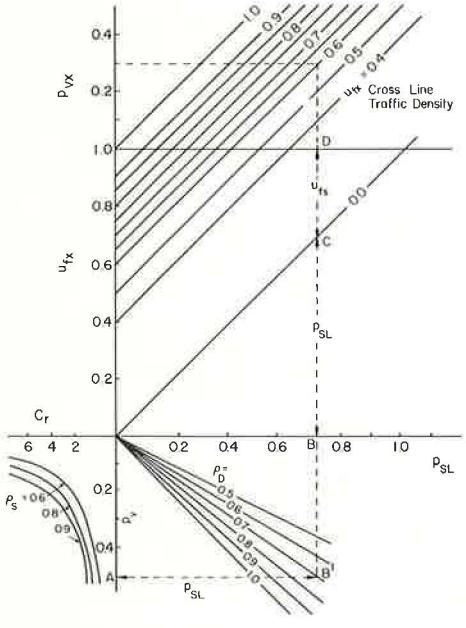

CONCLUSIONS

A PRT network has been designed to carry all internal automobile trips occurring in 1990 in a high-density large metropolis. The theoretical guideway capacities required are about 4 times those of freeway lanes. With line spacings of ¼, ½, and 1 mile in the CBD, inner city, and outer rings respectively for the network of 1-way routes, respective speeds of 20, 40, and 40 to 50 mph are feasible.

Stations using moving belts are recommended for high-capacity PRT systems having station capacities of 480 to 960 vehicles/hour. Such belt stations result in shorter platform lengths and smaller vehicle queues at stations. The geometric design of stations and intersections has assumed acceptable and conservative normal and centripetal acceleration and jerk rates.

The stations should be designed with 25 percent excess capacity, for only 80 percent use is possible. The stations should provide for accommodating a maximum of 4 to 6 vehicles on the upstream queuing zone and 2 to 3 vehicles on the downstream queuing zone. The average waiting time will be 20 to 30 sec on the upstream side and

less than 2.0 sec on the downstream side, and probability of rejection on the upstream side at peak time is 2 percent. At a guideway density of 0.85, the probability of forced switching at stations will be 1/250 at peak time.

For intersections, capacity ratios of 1.6, 2.0, and 3.0 were considered. The turns in a high-capacity PRT network cannot be designed for the same capacity as the guideways, for this will result in unacceptably large radii of curvature and superelevation. The intersection should accommodate a maximum of 5 vehicles on the upstream side of the turn and provide for a maximum waiting time of 18 s-cycles on the downstream side. A probability of rejection of 1/40 and probability of forced switching of 1/80 are feasible at peak time. To keep the feasible guideway density at 0.75 to 0.85, the turn ratio should be larger than 0.5 and as high as 0.75. The average waiting time at an intersection is less than 2.0 sec on the upstream side and 3.0 sec on the downstream side.

The trigger theory can also be used for vehicle merging with synchronous control strategy and will result in less maneuver zone length, less power required, and less inconvenience to passengers.

At present a 60-station PRT network operating under quasi-synchronous control is being modeled for simulation to determine possible average guideway density, average speed of travel, vehicle use, total waiting times and delays, and other operating data. The proposed simulation of the 60-station network will provide an opportunity to test various new ideas introduced in this project.

COMPARISON WITH PREVIOUS WORK

York (8) simulated a PRT network under quasi-synchronous control. The guideway capacity was 3,600 vehicles/hour. In the present paper theoretical guideway capacities of 7,000 to 8,000 vehicles/hour were considered realistic for the PRT to be an efficient alternative to the automobile.

Dais (4) used large centripetal acceleration and jerk rates, superelevation for switches, and small separation between the main line and the off-line in the geometric design of off-lines at stations and intersections. These are unacceptable to some transportation engineers. Lower rates are used in this paper.

A high-capacity PRT system requires station capacities of 480 to 960 vehicles/hour. Since use of taxi stations results in large vehicle queues, belt stations are preferred. Munson (9) simulated belt stations by using gates on the upstream and downstream sides. However, the relations between main-line and off-line capacities and velocities and gate spacing were not given. Munson did not treat the station problem as a queuing process, and the trade-offs possible among service rate, traffic density, queue zone length, and user costs were not considered.

In contrast with the approach used by Munson, the approach in this project involved detailed mathematical analysis and queues modeled as M/D/1-FIFO and G/M/1-FIFO. The influence of HIS capacity, traffic density, and number of triggers on excess capacity and queue zone length required, average block-circling time, and total waiting time has been considered, and the possible trade-offs have been analyzed. The probability and cumulative probability distributions of waiting time in queue and interarrival time on HIS have also been obtained.

Brill (10) modeled vehicle motion ahead of a bottleneck as a queuing model and obtained the distribution of slow-down points for a freeway system.

Munson (9) simulated an intersection with off-line capacity and speed the same as those for the main line, as used in a low-capacity, low-speed PRT system, and slot shifting that used repeated combined acceleration-deceleration maneuvers on the main line to reduce the probability of rejection. Such maneuvers require large excess power and result in much brake wear and passenger inconvenience. Dais (4) simulated intersections of the same capacity as the main line and assumed vehicle stopping on the off-line.

For the high-capacity PRT network in this project, intersection capacity is less than main-line capacity and slot slipping maneuvers are only on the off-lines. To prevent rejection of high-priority vehicles at the switch, forced switching is adopted at stations

and intersections. It constrains the number of downstream triggers, depending on sensing space available and the length of main line between switch and merge.

REFERENCES

1. An Evaluation of Alternative Land Use and Transportation Systems in the Chicago Area. Chicago Area Transportation Study, Oct. 1968.
2. Thangavelu, K. Analysis, Simulation, and Design of Stations and Intersections for a Quasi-Synchronous Personal Rapid Transit Network. Urban Systems Engineering Center, Northwestern Univ., Aug. 1973.
3. Dais, J. Minichanges, Stations and Geometry in PRT. National Conference on Personal Rapid Transit, Univ. of Minnesota, Minneapolis, Nov. 1971.
4. Dais, J. Geometric Design of PRT Network Elements. PRT Conference, Minneapolis, May 1973.
5. McFarland, R. A. Human Factors in High-Speed Ground Transportation With Special Reference to Passenger Comfort and Safety. Carnegie-Mellon Univ., Transportation Res. Rept. 3, Nov. 1969.
6. A Policy on Geometric Design of Rural Highways. AASHO, 1965.
7. Saaty, T. L. Elements of Queuing Theory. McGraw-Hill, New York, 1961, pp. 154-155.
8. York, H. Simulation of Vehicle Management Strategies. In New Concepts in Urban Transportation, Univ. of Minnesota, Vol. 2, No. 11 and No. 12.
9. Munson, A. V. Quasi-Synchronous Control of High Capacity PRT Networks. National Conference on Personal Rapid Transit, Univ. of Minnesota, Minneapolis, Nov. 1971.
10. Brill, E. A. A Model of Traffic Jam Behind a Bottleneck. Operations Research, Vol. 4, No. 4, July-Aug. 1972.